

Design And Verification of An Automated Pressure Mapping System and Modulating Air Cells for Pressure Ulcer Prevention

Thanawin Khajornwadthanakul¹, Surangsee Dechjarern²

¹M.Tech, student, Department of Production Engineering, King Mongkut's University of Technology North Bangkok, Bangkok, Thailand.

²Assistance Professor, Department of Production Engineering, King Mongkut's University of Technology North Bangkok, Bangkok, Thailand.

Abstract

Patients who are unable to help themselves and sleep on a regular mattress face an increased risk of pressure ulcers, especially elderly and bedridden patients. The external contact pressure on the mattress can lead to injuries when blood pressure exceeds that of the capillaries, disrupting blood supply to the capillary network and resulting in pressure ulcers. This occurs due to inadequate force distribution and poor air circulation between the skin and the mattress. This research focuses on developing an intelligent air mattress prototype based on commercially available alternating pressure air mattresses to prevent pressure ulcers. Force-sensitive resistors (FSRs) are installed under each air cell to measure interface pressure values occurring at different parts of the body. These collected values are then used to create pressure maps, indicating areas of high overpressure. The prototype incorporates a smart pneumatic control system divided into seven functional areas: head, back, waist, buttocks, thighs, calves, and heels. All operations are performed using LabVIEW software. Furthermore, all instruments have been calibrated and verified. To obtain the optimal pattern for cell expansion, inflation times in each cell were experimentally adjusted using a human model before conducting real human trials. Attention was primarily given to adjusting the growth rate in the back, buttocks, and calves, as these areas experience higher pressure compared to other parts of the body.

Keywords: Pressure ulcers prevention, Alternating Pressure Air mattress, Real-time interface pressure mapping, FSR, Air cell modulation

1. Introduction

A pressure ulcer is an injury to the skin or subcutaneous tissue, typically occurring on the hips, sacrum, coccyx, heels, and other areas. It is a common medical complication found in the elderly, paralyzed patients, individuals with limited mobility or exercise, and those who are bedridden [1-3]. This condition occurs due to prolonged pressure on the skin, resulting in impaired circulation of capillaries in the subcutaneous tissue [4, 5]. To distribute pressure and alleviate the risk of pressure ulcers, proper positioning of the patient or the use of an overlay, such as an Alternating Pressure Air Mattress (APAM) or seat cushion, is necessary. These commercially available devices feature air cells that inflate and deflate, effectively redistributing pressure [6-11]. However, these devices operate based on the present

system defined by the manufacturer and lack the ability to sense high-pressure areas. As a result, they may continue exerting pressure on already damaged or susceptible skin, making it challenging to reduce pressure distribution [12, 13]. To optimize these devices, improvements are required in both the control system and the recognition section. Typically, force-sensitive resistors (FSRs) are incorporated into the device, which measure pressure between the contact surfaces. FSRs are rectangular or circular in shape and highly sensitive to changes in resistance [14-17]. However, their performance can be affected by external electric fields, necessitating complex reading circuits such as capacitor amplifiers and resistors. The resistance sensor measures changes in the conductivity of the sensing material when it is pressed or subjected to physical force. These sensors have a thin and flexible structure, but their output signal is non-linear. A graphical user interface (GUI) is used to provide real-time pressure maps from commercial pressure monitoring pads in the supine position [18, 19].

2. System description and fabrication

2.1 Before you begin to format your paper, first write and save the content as a separate text file.

The system (Figure 1) comprises an alternating pressure air mattress (APAM), a control box, and a GUI. The mattress dimensions are 90 x 180 x 10 cm (W x D x H), with 22 air cells. Each cell is equipped with 2 sensors, functioning as both sensors and actuators for monitoring and adjusting the air cells. A mattress control box measures 22 x 55 x 55 cm (W x D x H) and consists of 3 layers. The lower layer contains 17 units of solenoid air valves (3/2 way). The middle layer includes a switching power supply DC24V, 4 units of long-life ultra-quiet medical micro air pumps, solid-state relay, terminal bar, and power plug, shown in Figure 2(a). However, due to the high interface pressure on the back, buttocks, and calves, separate air controls were implemented for the corresponding air cells in contact with the human body. Specifically, air cells 4 to 6 are assigned to the back, cells 9 to 12 to the bottom, and cells 16 to 19 to the calves. To regulate the air pressure and prevent damage, check valves and pressure transmitters were incorporated, ensuring that the bed's air pressure does not exceed 0.2 MPa. The upper layer of the control box consists of NI myRio, arduino mega, relay module and analog Multiplexer, shown in Figure 2(b).

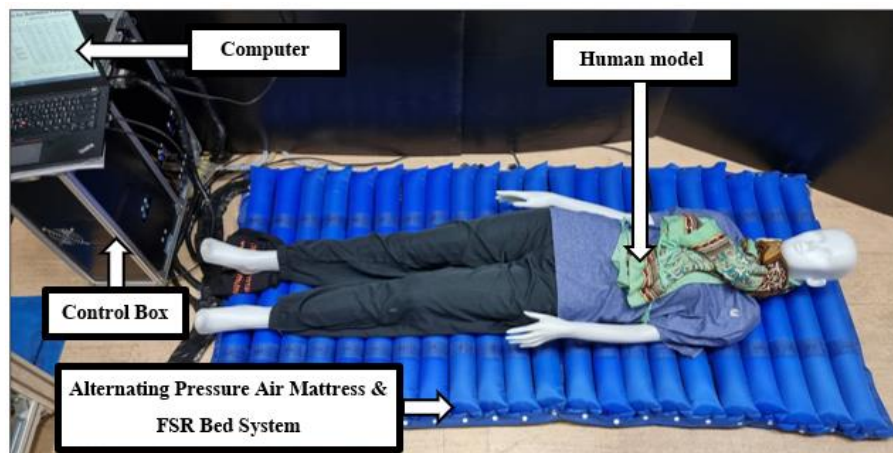


Figure 1: A human model laying down on alternating pressure air mattress with control box.

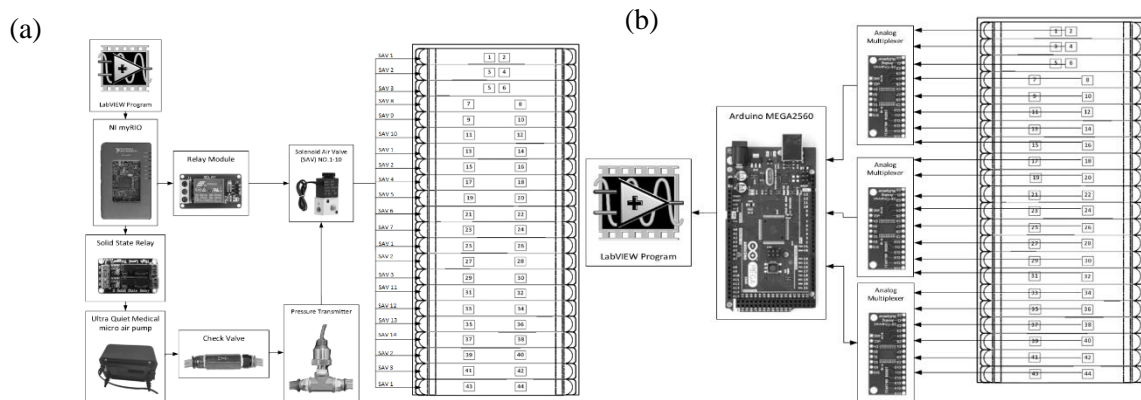


Figure 2: Schematic of (a) the pneumatic control system for alternating pressure air mattress and (b) the connections between FSR bed system and Arduino mega board.

2.2 Keep your text and graphic files separate until the text has been formatted and styled.

To ensure accurate monitoring, two force sensing resistors (FSRs) are installed under each air cell of the mattress, resulting in a total of 44 units, shown in Figure 3. The sensors are positioned parallel to the cell. The distance between the two sensors is maintained between 40 to 50 cm. To handle the significant number of inputs, 16-Channel Analog Multiplexers (CD74HC4067) are utilized to consolidate the analog signals. These multiplexers combine the sensor data before transmitting it to the Arduino Mega for further processing, shown in Figure 2(b). LabVIEW is employed to collect and analyze the data, determining whether each air cell needs to be inflated or deflated.

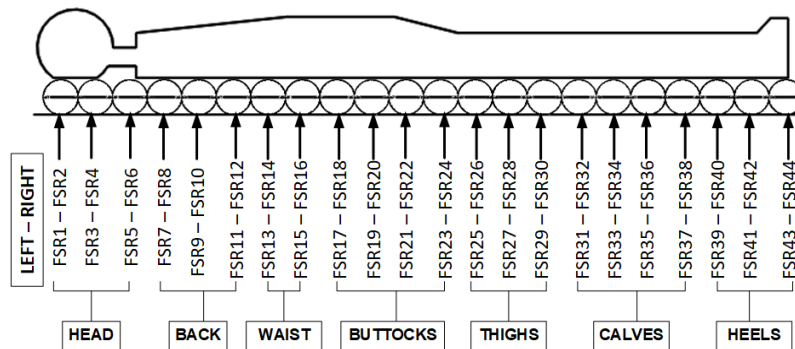


Figure 3: Scheme of the sensors under the air cell with the human body.

The LabVIEW program serves as the human-machine interface, allowing users to interact with the system. It is responsible for reading signals from the sensors, controlling the pneumatic system, processing data, and recording results. The program retrieves multiple values and combines them into an array, which is then displayed in the Intensity graphic. In this graphic, the transition from white to black indicates areas of high pressure. Users can also view specific pressure values at particular points and perform other related tasks. The GUI provides both automatic and manual modes. In automatic mode, the program selects the appropriate time for inflating or deflating each stage on its own. In manual mode, users have control over the timing of inflation or deflation at specific locations, allowing for more precise adjustments. The pressure values measured on different body parts, including the head, back, waist, buttocks, thighs, calves, and heels, are displayed. Experimental data is saved in the TDMS file format, ensuring convenient storage and access to the recorded information, shown in Figure 4.

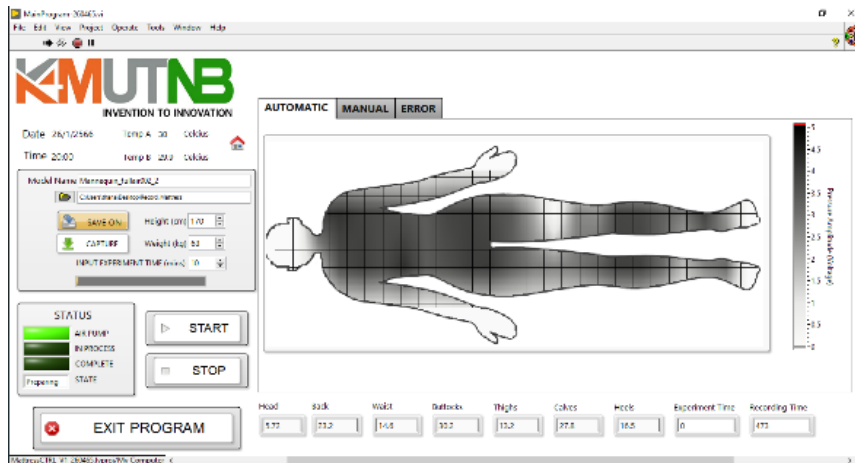


Figure 4: LabVIEW-based GUI for the operating and monitoring of the alternating pressure air mattress.

3. FSRs performance and implementation

3.1 Calibration and result.

In this study the FSR 406 model of Interlink Electronics was used, a polymer thick film sensor with 45 x 45 mm. It outputs from 0 - 5 volts. It needs calibration to convert the signal from volt to pascal for the output signal to be pressure (force/area). There were 4 calibration tools: Standard weight set (1 kg, 2 kg, 5 kg), FSR, Arduino MEGA and LabVIEW as shown in Figure 5.

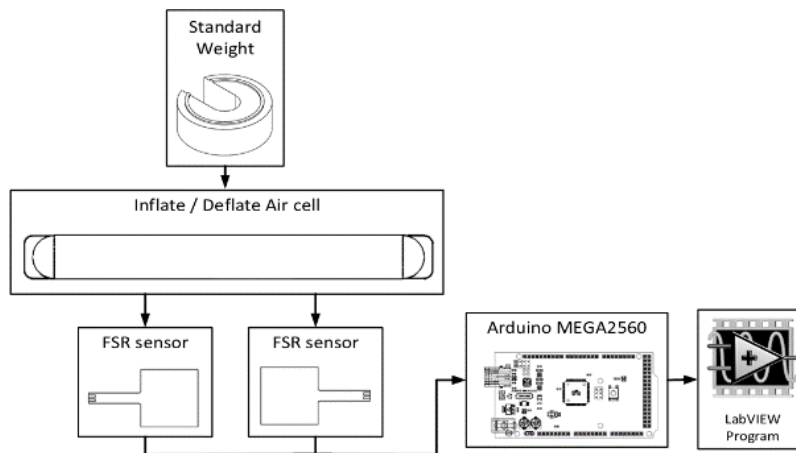


Figure 5: Schematic of performance test.

In calibration of sensor. Place a standard weight on the FSR and save the values. Repeat three times. Take weights of 1 kg, 2 kg, 3 kg, 4 kg and 5 kg respectively. Then find the mean (AVG) and standard deviation (SD).

Table 1: The mean values for actual pressure after standard weights are placed and converted to Pa.

Weight (kg)	Pressure (V)	Standard deviation
0	0.00	0.00
1	5.108	0.095
2	5.897	0.023
3	6.083	0.016
4	6.558	0.021
5	7.344	0.025

Calculate pressure in pascal unit (force/area) from standard weight set and cross-sectional area of sensor. The size of force sensitive resistor (FSR) is 0.12 and 0.30 (width x length). So the area is 0.036 m².

$$F = m \times g \tag{1}$$

$$P = F/A \tag{2}$$

Calculate the pressure at 1 kilogram by converting the unit to vector volume and convert the unit to pascal form, where 1 N/m² equal 1 pascal. Therefore, this is equivalent to 272.2 pascal or 0.2722 kilopascal. It was found that the obtained values tended to increase linearly, shown in Figure 6.

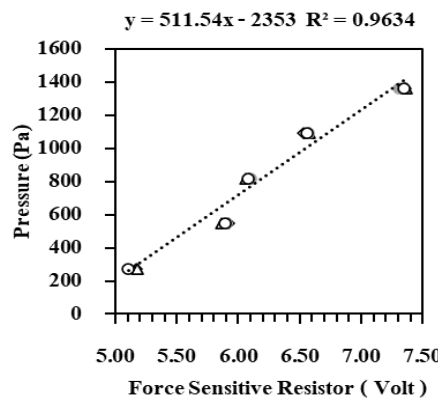


Figure 6: Comparison of the FSR with the calculation from the linear equation.

3.2 Verification and result.

From Table 2, it can be observed that the sensor exhibits a voltage that varies with increasing weight, following a straight-line equation. It demonstrates a maximum error of 4.18 at a weight of 1 kg and a minimum error of 0.48 at a weight of 4 kg, specifically for pressures below 3 kPa, which is lower than the pressure threshold associated with the risk of pressure sores. This verifies that the selected piezoresistive sensor is capable of detecting values within the interpolated range of capillary blood pressure in normal tissue. Additionally, it is evident that the sensor exhibits a good level of sensitivity to lower pressure values.

Table 2: The mean values from verification process.

Standard Weight (kg)	Calculated Pressure (Pa)	Actual Pressure (Pa)	SD	%Error
0	0.00	0.00	0.00	0.00
1	272.50	261.11	18.99	4.18
2	545.00	560.42	11.26	2.83
3	817.50	847.14	20.86	3.63
4	1090.00	1084.77	8.16	0.48
5	1362.50	1384.11	20.36	1.59

4. A human model

A mannequin resembling a female with a height of 170 cm was utilized to fine-tune the inflation timing and achieve the optimal pattern for the air cells. However, the mannequin's interior was empty, so to simulate a real human as accurately as possible, a significant amount of sand was introduced into the mannequin's body [20].

Table 3: Adjusted parameters for the human segment mass model.

Segment	Mass (%)	Calculated weight (kg)	Actual weight (kg)
Head	6.68	4.13	3.00
Trunk	42.57	26.35	21.92
Arms & Hands	8.98	5.54	4.14
Legs & Feet	41.76	25.84	33.53
Total	100	61.9	62.59

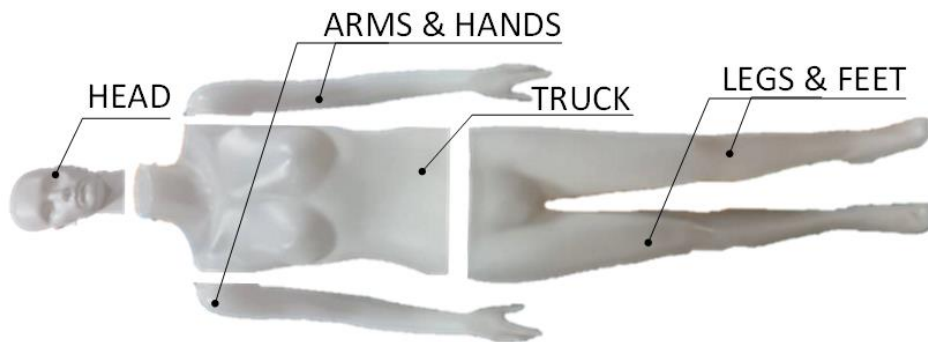


Figure 7: A human model segmentation.

5. Air cells modulation test

5.1 Pressure reduction and result analysis.

During the experiment, the inflation time for all 22 air cells of the mattress was determined. The process involved testing the time it took for each cell to reach full inflation. It was observed that at 400 seconds, all the cells were fully inflated. After that point, the expansion rate was adjusted to a predetermined percentage, gradually reducing it to 60%. To initiate the experiment, the user would press the "Start" button on the GUI. This action activates the air pump and solenoid valves, initiating the inflation process. Once the specified time has elapsed, the program automatically cuts off power to the air pump and solenoid valves, concluding the experiment. The results of the experiment, including the inflation times for each air cell, are then saved for further analysis and evaluation. The test involved using an air mattress, control box, GUI, and mannequin. The GUI commands were used to set the time, monitor the interface pressure, and control the pneumatic system. A computer running at a speed of 2.4 GHz was used to execute and initiate the experiment.

The time was set at different intervals: 400s, 360s, 320s, 280s, 240s, representing 100%, 90%, 80%, 70%, and 60% respectively. Once the specified time elapsed, the "Save" button was pressed to record the data. On the front panel, the areas of high interface pressure could be observed through the intensity graphic, which provided visual representations of pressure distribution across the head, back, waist, buttocks, thighs, calves, and heels. To avoid overloading the computer, the intensity graphic was saved as an image file, while the default program was saved in TDMS format. Manual conversion of the TDMS files to Excel files was necessary to obtain the numerical values of the interface pressure.

Table 4: Determine the time of inflated air cells

Expansion rate	Filling time(Second)
100%	400
90%	360
80%	320
70%	280
60%	240

From table 5, The analysis of the results from the five levels of air cell modulation revealed that when the expansion rate was set at 100%, the maximum interface pressure was observed at the back, buttocks, calves, and heels. As the time for inflation decreased, the interface pressure correspondingly reduced. This indicates a proportional relationship between inflation time and interface pressure.

According to the experimental results, the interface pressure on the back, buttocks, and calves were too high, so the pneumatic control on that area was separated to be controlled directly. Determined by the position of the air cell in contact with the body. The back has air cells number 4 to 6. The buttocks have air cells number 9 to 12. The calves have air cells number 16 to 19.

Table 5: The pressure mapping and measuring data when a human model used different air cells expansion rates.

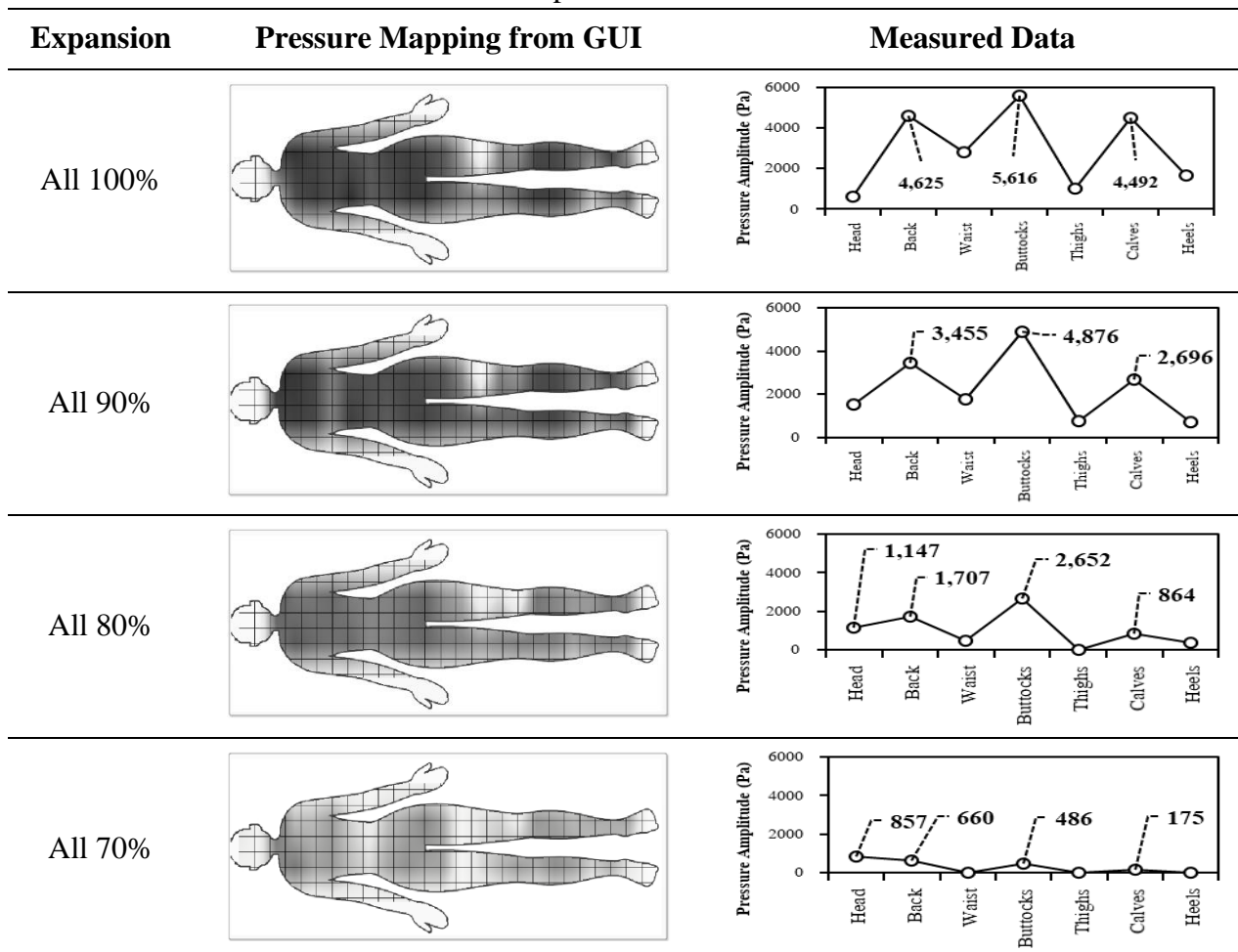
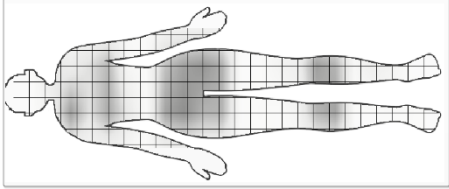
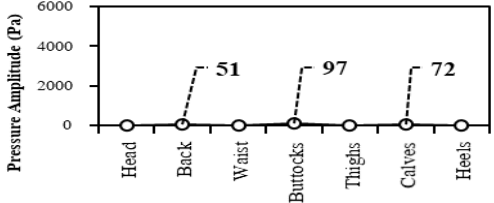


Table 5: The pressure mapping and measuring data when a human model used different air cells expansion rates (next).

Expansion	Pressure Mapping from GUI	Measured Data
All 60%		

5.2 Pressure distribution and result analysis.

This experiment was a continuation of the previous one, which aimed to test the pressure around the back, buttocks, and calves, as it was observed that the pressure in these areas was higher than in others. Therefore, the expansion rate was reduced to 80% and 60% specifically for these areas while keeping other areas of the body inflated to 100%.

During this experiment, the expansion rate was reduced to 80% and 60% simultaneously around the back, buttocks, and calves. The expansion rate was switched for each area to observe changes in depth. If the inflation rate is not the same across different areas, adjustments were made accordingly. However, it should be noted that other areas of the body remained fully inflated at 100%.

Table 6: Determine the expansion rate of inflated air cells.

Number	Position of human body						
	Head	Back	Waist	Buttocks	Thighs	Calves	Heels
1	100%	100%	100%	<u>80%</u>	100%	100%	100%
2	100%	100%	100%	<u>60%</u>	100%	100%	100%
3	100%	<u>80%</u>	100%	100%	100%	100%	100%
4	100%	<u>60%</u>	100%	100%	100%	100%	100%
5	100%	100%	100%	100%	100%	<u>80%</u>	100%
6	100%	100%	100%	100%	100%	<u>60%</u>	100%

According to the expansion rate of air-cells in table 6, number 1-2 interface pressure at the buttocks are significantly reduced with blow rate, shown in Figure 8(a). Numbers 3-4 in table 6, reduce the blow rate in the back area. The interface pressure on the back and calves are reduced, shown in Figure 8(b). But nothing happened in the buttocks. Numbers 5-6 in table 6, reduce the blow rate in the calves area. The interface pressure at the calves was greatly reduced and at the buttocks as well, shown in Figure 8(c). It can be concluded that if the human body interface pressure must be reduced. It must be done in combination with all three, not only the back, buttocks, or calves. The relationship between body segments and the effect of interface pressure amplitudes are shown in figure 9. After confirming that the isolated expansion of air cells locally in the back, buttocks and calves could not reduce the total interface pressure. It had to synchronize the expansion of the three section simultaneously.

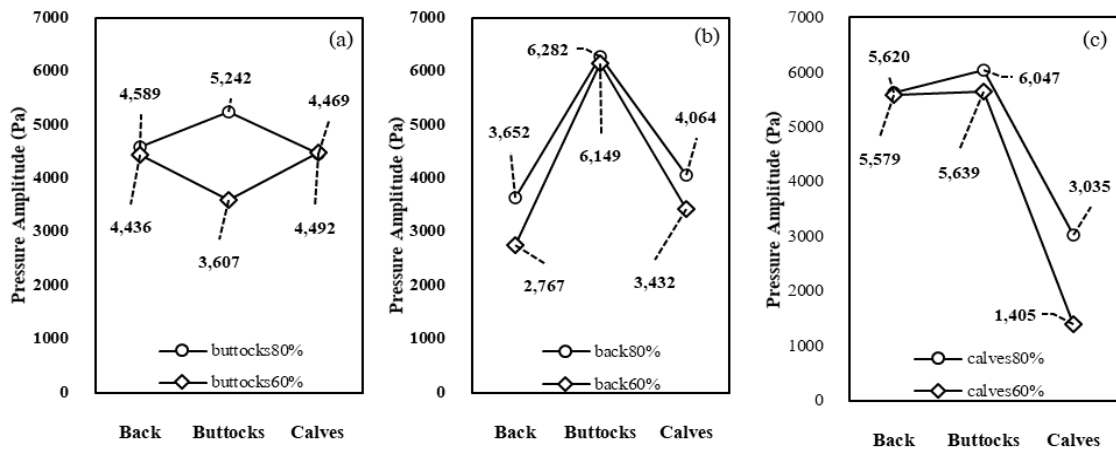


Figure 8: Relation chart between (a) interface pressure at the buttocks with an air-cells expansion rate of 80% and 60%, (b) interface pressure at the buttocks with an air-cells expansion rate of 80% and 60%, (c) interface pressure at the calves with air-cells expansion rates of 80% and 60%.

Table 7: Determine the expansion of air cells in the back, buttocks and calves.

Number	Position of human body						
	Head	Back	Waist	Buttocks	Thighs	Calves	Heels
1	100%	80%	100%	80%	100%	80%	100%
2	100%	80%	100%	80%	100%	60%	100%
3	100%	60%	100%	80%	100%	80%	100%
4	100%	60%	100%	80%	100%	60%	100%
5	100%	80%	100%	60%	100%	80%	100%
6	100%	80%	100%	60%	100%	60%	100%
7	100%	60%	100%	60%	100%	80%	100%
8	100%	60%	100%	60%	100%	60%	100%

According to the expansion rate of the air cells in table 7, number 1-4 limit the expansion of the buttocks air cells at 80%, then alternating expansion of the dorsal and calves air cells at 80% and 60% respectively. The results show that the alternating expansion of the air cells of the dorsal and calves areas is not important. Because the pressure interface of the buttocks changes very little, shown in Figure 9(a). In the other way, number 5-8 limit the expansion of the buttocks air cells at 60%, then alternating expansion of the dorsal and calves air cells at 80% and 60% respectively. The results were the complete opposite. The pressure interface on the buttocks were reduced and the pressure interface on the back and calves were reduced accordingly. When reducing the expansion of air cells in the area of the back and calves. It also lowers the pressure interface on the buttocks. The relationship between body segments and the effect of interface pressure amplitudes are shown in Figure 9(b).

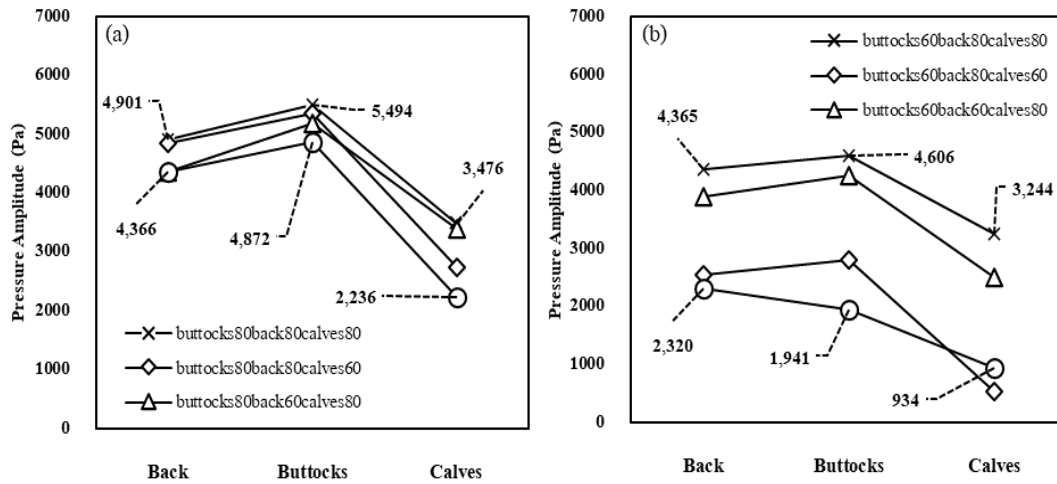


Figure 9: Relation chart between (a) interface pressure at the buttocks with an air-cells expansion rate of 80%, back and calves with alternating air-cells expansion rates of 80% and 60%, (b) interface pressure at the buttocks with an air-cells expansion rate of 60%, back and calves with alternating air-cells expansion rates of 80% and 60%.

6. Conclusions

In this study, a human model was used lying down on an alternating pressure air mattress with an FSR bed system and pneumatic control system. To mimic a real human, a substantial amount of sand was used to fill the mannequin according to its weight and proportions. During the test, the pressure between the interfaces of the mattress was continuously monitored in real time, and the GUI displayed pressure mapping and inflate times for the air cells. When all air cells were fully inflated to 100%, measurements of total body proportion were taken. It was observed that the pressure between the interfaces was particularly high in the buttocks, back, and calves. The study then focused on determining the rate of expansion of the air cells in those specific locations, with an emphasis on reducing the pressure between the interface formed in the buttocks. Initially, experimental adjustments were made by altering the expansion of the air cells at specific locations (e.g., back, buttocks, calves) while disregarding other areas. However, this approach proved ineffective as it led to an increase in pressure in the neglected areas, which was counterproductive. Subsequently, the experiment was adjusted to work collectively, determining the expansion rate of the air cells to function simultaneously but with different values to achieve the desired outcome. From the conducted experiments, it was concluded that in order to reduce the pressure between the interfaces of the buttocks, the rate of expansion of the air cells in the buttocks needed to be decreased first. Subsequent reductions were then made in the areas of the back and calves to achieve optimal results in reducing the pressure between the interfaces.

However, it's important to note that the human model used in the study had a rigid body and lacked the anisotropic properties of real human skin. This difference may impact the applicability of the parameters derived from the dummy to all individuals. Therefore, future advancements should focus on developing devices and programs that can predict and adapt air cell configurations to individual patients' needs and characteristics.

7. Acknowledgments

This research was facility supported by King Mongkut's University of Technology North Bangkok.

8. References

1. Tantirat P, Suphanchaimat P, Rattanathumsakul T, Noree T. Projection of the Number of Elderly in Different Health States in Thailand in the Next Ten Years, 2020–2030. *Int. J. Environ. Res. Public Health*. 2020;17(22):8703.
2. Gajanandana R. Aging society and driving the Thai economy [Internet]. Thailand: The secretariat of the house of representatives; 2018 [cited 2023 Aug 2]. Available form: <https://www.dop.go.th>.
3. Social statistics division. The 2021 survey of the older persons in thailand [Internet]. Thailand: National Statistical Office; 2022 [cited 2023 Aug 2]. Available form: <http://service.nso.go.th>.
4. Edsberg LE, Black JM, Goldberg M, McNichol L, Moore L, Sieggreen M. Revised National Pressure Ulcer Advisory Panel Pressure Injury Staging System. *J Wound Ostomy Continence Nurs*. 2016;43(6):585-597.
5. Lee W, Won BH, Cho SW. Finite element modeling for predicting the contact pressure between a foam mattress and the human body in a supine position. *Computer Methods in Biomechanics and Biomedical Engineering*. 2017;20(1):104-117.
6. Cho HS, Ryu JC, Kim GS, Mun MS, Kim KH, Lee IH. Analysis of Body Pressure Distributions of the Air-Cell Mattress for Preventing Decubitus Ulcer. *Key Engineering Materials*. (2006);326:743-746.
7. Ehelagastenna M, Sumanasekara I, Wickramasinghe H, Nissanka ID, Nandasiri GK. Design of an Alternating Pressure Overlay for the Treatment of Pressure Ulcers. 2021 Moratuwa Engineering Research Conference (MERCon); 2021 July 27-29; Moratuwa Sri Lanka. IEEE; 2021. p. 202-207.
8. Ishibashi Y, Matsumiya R, Ohno K, inventors; Paramount Bed Co, Ltd, assignee. United States patent US 9,597,244 B2. 2017 Mar 21 [cited 2023 Aug 2]. 22 p. Available from: <https://patents.google.com/patent/US9597244B2>.
9. Change ML, Hsieh M, Cheng WC, Lee PK, Liu YC, Chou FJ, inventors; Apex Medical Corp, assignee. United States patent US 11,197,794 B2. 2021 Dec 14 [cited 2023 Aug 2]. 23 p. Available from: <https://patents.google.com/patent/US11197794B2>.
10. Moon I, Kang SJ, Kim GS, Mun MS. A Novel Air-cell Mattress Based on Approximate Anthropometric Model for Preventing Pressure Ulcer. International conference on Control, Automation, and Systems (ICCAS); 2005 June 2-5; Gyeonggi-Do, Korea. ICCAS; 2005. p. 1278-1282.
11. Chai CY, Sadou O, Worsley PR, Bader DL. Pressure signatures can influence tissue response for individuals supported on an alternating pressure mattress. *Journal of Tissue Viability*. 2017;26(3):1-9.
12. Lee KH, Kwon YE, Lee H, Lee Y, Seo J, Kwon O, Kang SW, Lee D. Active Body Pressure Relief System with Time-of-Flight Optical Pressure Sensors for Pressure Ulcer Prevention. *Sensors*. 2019;19(18):3862.
13. Kawabata T, Sugama J. Relationship between mattress internal air pressure and interface pressure distribution in the lateral position. *Int Wound J*. 2022;19(8):2115-2123.
14. Pranjoto H, Sarwono WC, Miyata AF, Agustine L. Raspberry Pi-based Decubitus Reducing Mattress with Air pressure Monitoring System and Air Leaks Detector. 4th Int. Con. Computer and Informatics Engineering (IC2IE); 2021 Sep 14-15; Depok Indonesia. IEEE; 2021. p. 418-423.

15. Pereira S, Simoes R, Fonseca J, Carvalho R, Almeida J. Design and development of an embedded sensors matrix for pressure mapping and monitoring applications. *Microprocessors and Microsystems*. 2020;74:103004.
16. Kwong E, Pang G. Development of an Intelligent Seat for the Alleviation of Pressure Ulcers. 11th Biomedical Engineering Int. Con. (BMEiCON); 2018 Nov 21-24; Chiang mai Thailand. IEEE; 2018. p. 1-5.
17. Carrigan W, Nuthi P, Pande C, Wijesundara MJB, Cheng-Shiu Chung, Grindle GG, Brown JD, Gebrosky B, Cooper RA. Design and operation verification of an automated pressure mapping and modulating seat cushion for pressure ulcer prevention. *Medical Engineering and Physics*. 2019;69:17–27.
18. Qidwai U, Al-Sulaiti S, Ahmed G, Hegazy A, Ilyas SK. Intelligent Integrated Instrumentation Platform for Monitoring Long-term Bedridden Patients. 2016 IEEE EMBS Conference on Biomedical Engineering and Science (IECBES); 2016 Dec 4-8; Kuala Lumpur Malaysia. IEEE;2016. p. 561-564.
19. Matar G, Lina JM, Kaddoum G. Artificial neural network for in-bed posture classification using bed-sheet pressure sensors. *IEEE J Biomedical and Health Informatics*. 2018;24(1):2168-2194.
20. P De Leva. Adjustments to Zatsiorsky-Seluyanov's segment inertia parameters. *J Biomechanics*. 1996;29(9):1223-1230.